Proceedings of the 2025 Winter Simulation Conference
E. Azar, A. Djanatliev, A. Harper, C. Kogler, V. Ramamohan, A. Anagnostou, and S. J. E. Taylor, eds.

OPERATIONAL SIMULATION OF MULTI-FUNCTIONAL CHARGING STATION FOR SUSTAINABLE TRANSPORTATION

Jeremiah Gbadegoye[1], Yang Chen[2], Olufemi A. Omitaomu[2], and Xueping Li[1]

[1] Dept. of Industrial and Systems Eng., The University of Tennessee, Knoxville, TN, USA
[2] Computational Sciences and Eng. Division, Oak Ridge National Lab., Oak Ridge, TN, USA

ABSTRACT

As transportation systems move toward electrification and decarbonization, multifunctional charging stations (MFCS) are emerging as key infrastructure for electric vehicles (EVs) and hydrogen fuel cell vehicles (HFCVs). This paper presents a simulation model of an MFCS that integrates solar photovoltaic (PV), wind power, battery storage, hydrogen (H_2) production, dual-pressure H_2 storage, fuel cells, and dynamic grid interactions. The model simulates daily operations using 5-minute resolution data to capture real-time variability in renewable energy (RE), demand, and electricity prices. A flexible dispatch algorithm dynamically allocates energy for EV charging, H_2 production, storage, and grid transactions while respecting system constraints. Results show that the MFCS effectively prioritizes RE usage, minimizes waste, meets diverse energy demands, and achieves net operational profit. The model serves as a valuable decision-support tool for designing and optimizing integrated clean energy hubs for zero-emission transportation.

1 INTRODUCTION

The global transition toward zero-emission transportation like EVs and HFCVs is driving the development of next-generation charging and refueling infrastructure. Multifunctional Charging Stations (MFCSs) have emerged as a promising solution by integrating EV charging, hydrogen (H_2) refueling, and potentially battery-swapping operations within a single facility (Zhang et al. 2025). These stations typically combine various energy systems (Xiao et al. 2025), this could include components such as PV, wind energy, battery energy storage systems, H_2 production by electrolysis of water, and interaction of the electricity grid to optimize energy utilization and operational cost. However, managing the dynamic interactions between these heterogeneous energy carriers and infrastructure components remains a significant technical challenge. A central complexity in MFCS operation arises from the variability of RE sources and the need for real-time balancing of generation and demand. Unlike conventional grid-tied stations, MFCSs operate in a more dynamic and constrained environment, where generation profiles are uncertain and H_2 production, compression, and storage must be actively coordinated to meet both immediate and future demand (Ramkumar et al. 2025). This complexity is amplified in intermodal logistics necessitating infrastructure to support medium and heavy-duty transport (Bogdanov et al. 2024). Effective MFCS design therefore requires a systems-level approach that captures the interplay between physical processes, energy conversion and storage technologies, market dynamics, and control strategies (Shi et al. 2024).

Substantial prior research has explored individual components of MFCS, including EV charging infrastructure planning, battery energy storage system (BESS), and H_2 refueling logistics. For instance, Sing et al. (2022) developed a hybrid simulation framework combining system dynamics and discrete-event modeling to evaluate workplace EV charging integrated with solar PV and batteries, demonstrating high levels of energy self-sufficiency. Complementing this, Benz and Pruckner (2023) applied optimization-based load shifting and showed that coordinated smart charging strategies can outperform or augment BESS investments when aligned with solar availability. Building on these efforts, recent studies have introduced data-driven control strategies for managing multi-energy systems; for example, Shi et al. (2024) proposed a

framework combining long short-term memory networks for forecasting with deep reinforcement learning for real-time decision-making in PV-battery-EV charging hubs. Efforts to simulate H_2-integrated infrastructure are also growing. Lee et al. (2024) conducted a techno-economic assessment of hybrid PV-wind-based MFCSs with H_2 production, while Wang et al. (2024) proposed a multi-stage co-optimization framework for electricity-H_2-transportation networks under decarbonization constraints. Discrete-event simulation approaches have also been applied as shown by Ait Alla et al. (2024) that increasing H_2 refueling speeds has a more pronounced impact on system throughput than increasing the number of stations, highlighting the value of detailed simulation in infrastructure design. Electricity market participation adds another layer of complexity to MFCS operations. Zheng et al. (2025) reviewed tariff- and aggregator-based models for grid interaction, emphasizing the potential of vehicle-to-grid integration to support demand-side flexibility. In another study, Zheng and Wei (2025) developed a real-time, prediction-free framework for peer-to-peer (P2P) energy trading using Lyapunov optimization, achieving near-optimal energy and cost balance without reliance on forecasts. Advanced dispatch algorithms are also being applied to optimize energy flows in distributed systems. Koenemann et al. (2024) trained artificial neural networks via reinforcement learning to outperform model predictive control under uncertainty. For risk-aware scheduling, Valipour et al. (2024) employed Entropic Value-at-Risk (a coherent risk measure that uses exponential utility to emphasize sensitivity to extreme losses) to manage uncertainty in prices and RE availability, improving system resilience. Simulation frameworks have also been applied in rural and off-grid settings: Ghirardi et al. (2024) used Transient System Simulation (TRNSYS) to explore the role of H_2 and EV flexibility in decentralized energy systems, achieving low levelized costs and high operational independence.

Despite these advances, few existing models fully integrate PV, wind, battery storage, electrolyzers, compressors, dual-pressure H_2 storage, fuel cells, and dynamic grid-market interactions into a unified simulation framework. Most approaches either simplify component behavior or omit key interactions such as H_2 compression or battery dispatch for H_2 production. To address this gap, this paper presents a modular, simulation framework for evaluating the operation of multifunctional charging stations under realistic temporal and economic conditions. We simulate a fixed operational period, incorporating RE variability, component-level constraints, EV and HFCV demand, and electricity price dynamics. Dispatch strategies are used to prioritize RE use, satisfy charging and refueling demands, and participate in grid markets. Energy flows, storage levels, and economic outcomes are tracked at high resolution, providing a detailed basis for evaluating system performance and infrastructure trade-offs. While prior work addresses individual elements of MFCS, none combine dual-pressure H_2 storage, electrolyzer dispatch, battery-grid-market interactions, and component-level constraints into a unified simulation. Our approach advances the literature by integrating these dimensions into a cohesive, high-resolution simulation model.

This work makes two key contributions: (1) a detailed simulation model capturing the physical and operational dynamics of an MFCS, and (2) a case study demonstrating its use in guiding the design, sizing, and economic dispatch of future clean energy hubs for zero-emission transport. The remainder of the paper is as follows: Section 2 describes the system and simulation framework; Section 3 outlines the case study and experiments; Section 4 presents results and insights; and Section 5 concludes the paper.

2 SYSTEM SCHEME AND DISPATCH STRATEGY

This section presents the architecture and energy dispatch logic of the MFCS designed to support both EVs and HFCVs, while dynamically participating in electricity market. Figure 1 provides a schematic overview of the station's architecture and the integrated energy pathways in the simulation. The MFCS is primarily powered by hybrid RE sources: solar PV and wind turbine whose variable output serves as the main energy supply for downstream operations. To manage this variability, the system incorporates a flexible BESS and hydrogen infrastructure, enabling both temporal energy shifting and cross-vector conversion.

The MFCS dispatch algorithm balances RE generation, energy demand, and market conditions at each time step (see Algorithm 1). Dispatch actions follow a prioritized sequence: serve HFCV demand from high and low pressure H_2 storage, charge EVs using RE, then battery discharge, and grid electricity if the

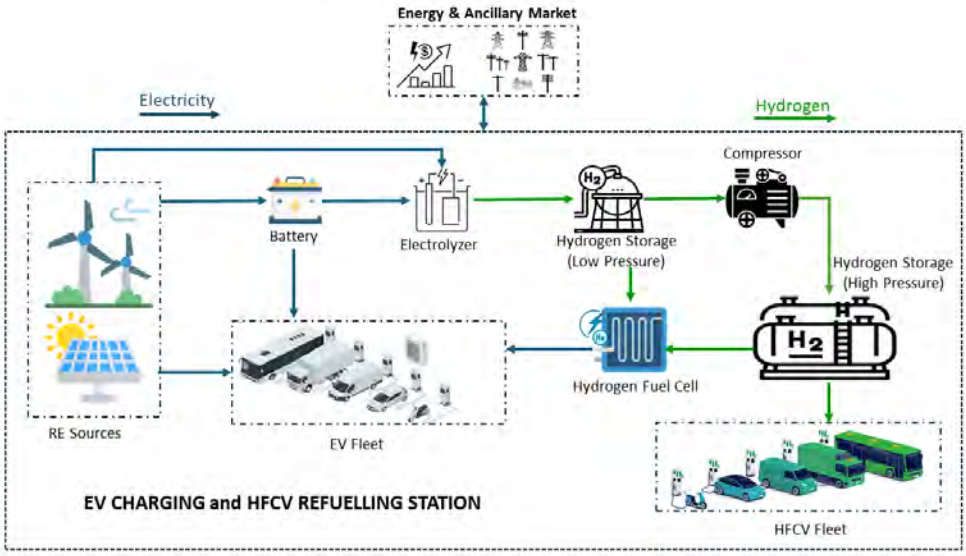

Figure 1: Schematic overview of the multifunctional charging station (MFCS) and grid interaction.

price P_t is acceptable. Fuel cell output is used as a last resort. Surplus RE supports battery charging or hydrogen production. Grid or battery power may supplement H_2 production, subject to system constraints. Parameters include: P_{grid} denotes the EV charging power from grid; P_{charge} indicates the battery charging power; P_{fuelcell} is fuel cell power output; P_{H2grid} is the power used by the electrolyzer for H_2 production from grid; and P_{sell} refers to the power exported to the grid. The control parameters include θ_{H2}, which sets the dispatch threshold for high-pressure H_2 storage, and θ_{compress}, regulates when H_2 is compressed from low- to high-pressure tanks. Dispatch decisions are logged continuously for system evaluation.

Solar output is determined using Equation (1), where PV power P_{PV} depends on panel efficiency η_{PV}, area A, and solar irradiance G_t (Huang et al. 2013). Wind power is computed by Equation (2), which incorporates air density ρ, rotor swept area A_r, power coefficient C_p, and wind speed v as derived in (Choukulkar et al. 2016). These generation outputs are dynamically allocated to subsystems based on operational state and market conditions, ensuring efficient and adaptive dispatch throughout the simulation.

$$P_{\text{PV}} = \eta_{\text{PV}} \cdot A \cdot G_t \tag{1}$$

$$P_{\text{wind}} = \frac{1}{2} \cdot \rho \cdot A_r \cdot C_p \cdot v^3. \tag{2}$$

The BESS enables temporal energy shifting and serves as a strategic buffer within the MFCS. It charges from RE sources or the grid when electricity prices are low, and discharges to support EV charging, H_2 production, or sell to the grid when prices are favorable. The model accounts for charging and discharging efficiencies, power rate limits, and a state-of-charge (SOC) reserve to protect long-term battery health. Charging and discharging decisions are driven by real-time conditions such as generation surplus, market price, e.t.c, allowing the BESS to dynamically balance short-term fluctuations and improve efficiency.

Hydrogen is produced via electrolysis using electricity sourced from RE, the battery, or the grid. The H_2 mass produced, m_{H_2}, is given in Equation (3), which relates input power P_e, electrolyzer efficiency η_e, and the lower heating value (LHV) of H_2 (Meier 2014):

$$m_{H_2} = \frac{\eta_e \cdot P_e \cdot \Delta t}{\text{LHV}_{H_2}}. \tag{3}$$

Produced H_2 is first stored in a low-pressure buffer tank, then compressed and transferred to a high-pressure vessel for HFCV refueling. Additionally, H_2 may be converted back to electricity using a proton

Algorithm 1 Operational Dispatch Algorithm for Multifunctional Charging Station (MFCS).

for each time step t **do**
  Input: Renewable generation (G_t), EV demand (D_t^{EV}), HFCV demand (D_t^{H2}), electricity price (P_t)
  Step 1: Serve HFCV demand using H_2 from high-pressure storage
  Step 2: Serve EV demand in the following order:
    (1) Use available renewable power (G_t)
    (2) Discharge battery
    (3) Purchase from grid if $P_t \leq P_{\text{grid}}$
    (4) Use fuel cell to convert H_2 to electricity if $P_t \geq P_{\text{fuelcell}}$
  Step 3: Charge battery with excess renewable power
  if battery has space **and** $P_t \leq P_{\text{charge}}$ **then**
    Charge battery from grid (limit to avoid overcharging)
  end if
  Step 4: Produce H_2 with surplus energy via electrolyzer
    (1) Use renewable power first (up to electrolyzer capacity)
    (2) Discharge battery only if high-pressure H_2 storage $< \theta_{\text{H2}}$
    (3) Use grid power if $P_t \leq P_{\text{H2grid}}$ and capacity allows
  Step 5: Store produced H_2 in low-pressure tank
  if low-pressure tank level $> \theta_{\text{compress}}$ **then**
    Compress and store in high-pressure tank
  end if
  if battery SOC $>$ reserve **and** $P_t \geq P_{\text{sell}}$ **then**
    Sell battery power to grid
  end if
  if surplus renewable remains and all internal needs are satisfied **then**
    Export RE to grid (up to limit)
  end if
  Step 6: Log all flows: EV/HFCV service, SOC, H_2 levels, grid activity, revenues, and costs
end for

exchange membrane (PEM) fuel cell. This conversion is described in Equation (4), where E_{FC} represents the energy output as a function of H_2 mass and fuel cell efficiency η_{fc}. This reversible pathway extends the flexibility of the MFCS by allowing stored H_2 to serve electricity demand under specific conditions.

$$E_{\text{FC}} = \eta_{\text{fc}} \cdot m_{H_2} \cdot \text{LHV}_{H_2}. \tag{4}$$

The MFCS interacts with the grid based on dynamic price signals. Grid imports are allowed only when internal generation is insufficient and prices fall below a threshold P_{buy}. Conversely, exports occur when RE is surplus, battery SOC exceeds reserve, and prices exceed P_{sell}. This economic layer ensures that every dispatch action is cost-effective and environmentally favorable. Grid electricity is also used for production when prices permit and storage needs persist. Any residual renewable surplus is exported to minimize curtailment and maximize environmental performance.

3 EXPERIMENTAL SETUP

To demonstrate the real-world applicability of the proposed simulation framework, we conducted a 7-day case study based on realistic operating conditions in the state of California. The aim is to evaluate the MFCS performance in optimizing RE utilization, reducing operational costs, and maintaining resilience under variable energy and demand conditions. The case study simulates integrated energy flows involving

EV charging, refueling, and grid participation, under fluctuating weather and market scenarios. This setup mirrors practical challenges faced by energy hubs co-located at intermodal or logistics hubs in urban regions.

3.1 Data Sources and Preprocessing

Environmental and market data were collected from publicly available sources and processed to align with the simulation timeline. Real solar irradiance and wind speed data were obtained from Weather Underground (Weather Underground 2025), capturing 5-minute interval observations over a full operational week. These measurements form the dynamic inputs for the PV and wind turbine generation subsystems. Electricity prices were sourced from CAISO's SP-15 (Energy) node (U.S. Energy Information Administration 2025), also provided at a 5-minute resolution in Pacific Time. This high temporal granularity ensures realistic modeling of time-sensitive electricity transactions, such as grid charging, selling, and hydrogen production. To maintain interpretability of the visualization, price spikes exceeding \$200/MWh were removed from the plotted data. Figure 2(a) illustrates the pronounced diurnal and intra-day volatility of the electricity market over the simulation period.

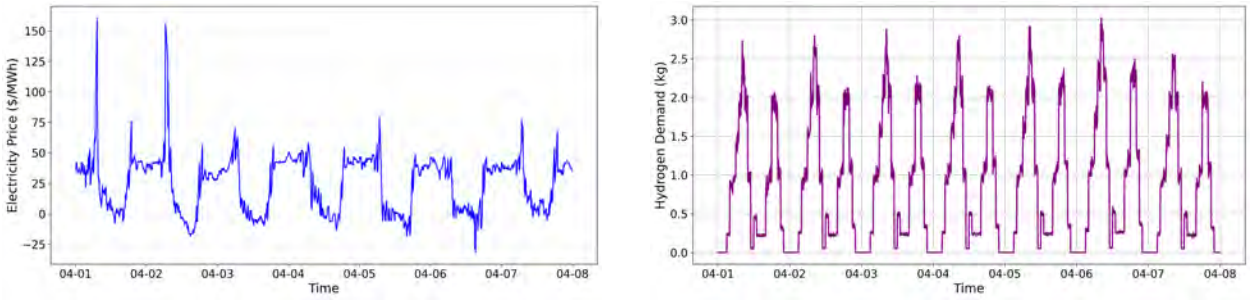

(a) Electricity price over the simulation week.

(b) Baseline hydrogen demand profile.

Figure 2: Time-series inputs used for simulation, based on real price and demand data.

Energy demands were synthesized from a combination of real and modeled data. EV arrivals are modeled as a stochastic Poisson process with a base rate of 3 vehicles per hour, modulated by a time-of-day profile to reflect realistic commuter patterns. Peak arrivals occur between (7:00–10:00 AM) and late afternoon (4:00–7:00 PM). At each timestep, the number of arriving EVs is sampled based on the current scaled rate. Each arrival is assigned a battery capacity (uniformly sampled from 60, 80, or 120 kWh), an initial SOC sampled from 10% to 90%, and a target SOC sampled between 90% and 100%. The charging demand is computed as the energy required to reach the target SOC from the initial SOC, accounting for individual variations. In contrast, HFCV demand was derived directly from a dataset (see Figure 2(b)) that included both arrival times and refueling quantities, eliminating the need for synthetic modeling of station-level behavior. All datasets were preprocessed to ensure temporal alignment throughout the simulation horizon.

3.2 Simulation Configuration

It is assumed that the modeled MFCS integrates 2500 m² of photovoltaic panels with 20% efficiency, 10 wind turbines each rated at 250 kW, and a battery system with 5000 kWh of capacity, 90% round-trip efficiency, and a 20% SOC reserve. H_2 is produced via a 5000 kW electrolyzer (0.7 kg/kWh efficiency), compressed using 1.0 kWh/kg and stored in two 100 kg tanks (low and high pressure). The fuel cell provides up to 100 kW at 50% efficiency, and the station interfaces with the grid under 20 MW purchase and 200 kW sell constraints, with buy/sell price thresholds of 50/70 \$/MWh. Ten EV chargers are available and used across most sensitivity scenarios. These settings reflect a medium-scale MFCS capable of both grid-interactive operation and standalone service continuity under moderate to high demand.

To evaluate the robustness and adaptability of the MFCS under variable conditions, a series of sensitivity experiments were conducted. These experiments were designed to isolate key parameters of the system and external drivers, such as volatility of electricity prices, fluctuations in EV traffic, and H_2 demand growth, and to assess their influence on system behavior, operational constraints and economic performance. The simulation framework was developed in Python as a discrete-time model with 5-minute resolution, enabling high-fidelity tracking of system dynamics and resource flows.

Table 1: Summary of experimental design and objectives.

Experiment Set	**System Variable**	**Objective and Insight**
Electricity Price Variation	Electricity price varied from -20% to $+20\%$	Examine impact of market fluctuations on grid transactions, hydrogen production, and profitability.
EV Arrival Rate Sensitivity	EV arrival rates adjusted (increased/decreased) with chargers fixed at 10	Analyze system congestion and service quality under fluctuating demand, using metrics like EV wait time and abandonment.
Charger Capacity Analysis	Number of chargers varied (arrival profile fixed)	Identify saturation effects and evaluate when additional chargers no longer significantly improve reliability. Supports infrastructure sizing.
Hydrogen Demand Stress Test	Hydrogen demand scaled up by 5% to 20%	Test production and storage capacity limits under growing demand. Quantify unmet demand and revenue loss to inform planning.

Each experiment modifies one variable at a time while keeping other conditions fixed, ensuring comparability across scenarios. In the simulation, EVs are considered abandoned if they wait more than 30 minutes for an available charger, capturing user tolerance thresholds and their effect on service quality. The baseline configuration was held constant across all runs, including a 7-day period of weather and electricity price data, enabling consistent evaluation of outcomes. Table 1 summarizes the four experiment sets, what was varied in each, and the corresponding insights these tests were designed to generate.

4 RESULTS AND DISCUSSION

4.1 Baseline Results

The RE generation profile is presented in Figure 3. Solar production exhibits a clear diurnal pattern, peaking around midday and dropping to zero overnight. In contrast, wind generation displays more stochastic behavior and often complements PV output, especially during early mornings and late evenings. The plot highlights how wind and solar contribute variably to the station's energy supply throughout the week. On some days, wind peaks significantly, surpassing 1 MW in short bursts, while solar provides a more stable and predictable contribution during daylight hours. This complementarity enhances the overall availability of RE but also necessitates advanced energy dispatch strategies. For instance, surplus solar during midday hours enables battery charging and production, while overnight wind generation helps reduce dependence on grid energy. These patterns emphasize the importance of hybrid RE integration and the real-time energy prioritization logic embedded within the MFCS.

In addition to electricity dispatch, the MFCS converts surplus energy into green H_2 through electrolysis. Figure 4a illustrates the daily production by source: renewables, battery discharges, and the grid. While renewables and batteries contribute meaningfully, grid electricity consistently supports over 100 kg/day of H_2 production, not as a fallback but as a strategic complement. This reflects the system's dynamic prioritization: RE is first allocated to EV charging, and H_2 production draws on remaining capacity or, when needed, on the grid, especially during periods of low electricity prices. Battery power further supplement H_2 production when marginal RE remains but is insufficient to fully power the electrolyzer.

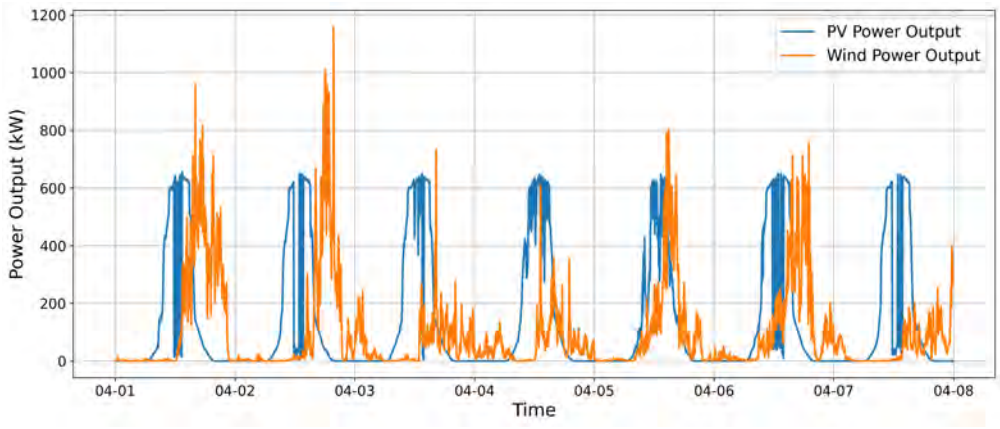

Figure 3: Solar and wind power over the 7-day simulation period for the studied location in California.

Figure 4b offers a grouped bar chart contrasting H_2 production by source with end-use destinations. Of the total H_2 produced, the grid supplies the largest portion (over 1000 kg), followed by renewables (over 600 kg), while battery support remains modest. Utilization is dominated by HFCV refueling, with only a minimal fraction directed to the fuel cell for electricity generation. Notably, the alignment between total H_2 produced and used H_2 indicates effective management of H_2 production-storage-refueling cycles.

To synthesize system-wide operational performance and economic outcomes, Table 2 presents a daily breakdown of key metrics. This includes RE generation totals, H_2 production disaggregated by source, battery charge/discharge energy, grid interactions, and financial indicators. A consistent trend is evident across the week: while total RE generation remains substantial (averaging over 5600 kWh/day), H_2 production from the grid persistently exceeds other sources, accounting for more than 50% of total production on most days.

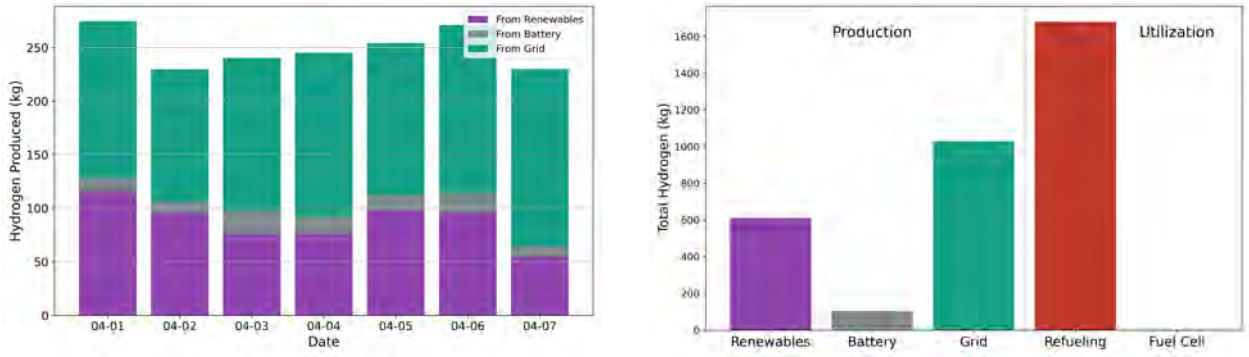

(a) Daily production by source.

(b) Cumulative production vs. utilization.

Figure 4: Overview of production sources and end-use distribution in the MFCS.

This outcome is directly tied to the system's dynamic grid participation logic and real-time pricing signals. Notably, despite the system's RE-first prioritization, the MFCS often purchases large amounts of electricity from the grid, with daily imports consistently over 1100 kWh and peaking above 1400 kWh. This behavior may seem counterintuitive for a RE-oriented system, but it reflects the strategic exploitation of *negative electricity prices* that occasionally arise in wholesale energy markets, especially in CAISO market with redundant solar power. During such periods, grid electricity is not only inexpensive but effectively *subsidized*, creating strong economic incentive to charge the battery and run the electrolyzer.

The data confirms this: on days when grid production is high (e.g., April 1 and April 7), grid purchases also spike, and yet the net economic outcome remains positive. For instance, on April 1, despite 1247.92 kWh

Table 2: Summary of daily MFCS operational and economic metrics.

Date	**H_2 Produced (kg) from power source**				**Grid Interaction (kWh)**		**RE Generation (kWh)**		
	RE	Battery	Grid	Total	Buy	Sell	PV	Wind	Total
1-Apr	115.52	13.01	146.14	274.67	1247.92	41.67	3309.30	3588.61	6897.91
2-Apr	95.26	11.03	123.39	229.68	1448.17	45.79	2948.03	2843.66	5791.69
3-Apr	75.72	22.03	142.64	240.39	1254.00	41.67	3667.33	1558.50	5225.83
4-Apr	76.11	15.98	153.14	245.23	1216.00	0.00	3501.91	1440.27	4942.18
5-Apr	98.22	14.19	141.76	254.17	1225.50	41.67	3093.26	2523.85	5617.11
6-Apr	95.94	18.46	156.64	271.04	1301.50	0.00	3135.94	3026.73	6162.67
7-Apr	54.50	10.04	165.39	229.93	1131.87	125.00	2961.99	1147.86	4109.85
Date	**Power Usage (kWh)**		**Battery Flow (kWh)**		**Revenue and Cost Breakdown ($)**				
	EV	H_2	Charge	Discharge	EV Rev	H_2 Rev	Grid Sell	Grid Buy	Net
1-Apr	1619.82	13078.30	1235.00	870.54	372.56	3395.09	3.16	-12.09	3758.72
2-Apr	1669.66	10935.86	1444.00	980.34	384.02	3804.08	4.19	-8.06	4184.23
3-Apr	2066.67	11445.60	1254.00	1536.44	475.33	4049.00	2.94	-1.79	4525.48
4-Apr	1693.33	11676.22	1216.00	1135.70	389.47	4051.55	0.00	-4.95	4436.07
5-Apr	1350.00	12102.31	1225.50	1126.86	310.50	4135.55	3.31	-1.01	4450.38
6-Apr	2013.33	12905.54	1301.50	1297.88	463.07	4465.32	0.00	-4.67	4923.72
7-Apr	2173.33	10948.08	1130.50	1260.19	499.87	3844.73	9.18	-9.47	4344.31

of grid imports and only 41.67 kWh of grid export, the MFCS still achieves a net profit of $3758.72. This demonstrates the station's ability to monetize low-cost grid electricity through sales and EV charging revenue. The observed profitability is further bolstered by the system's ability to avoid grid purchases during peak price periods and by its responsive scheduling of compression and battery charging operations.

Additionally, the battery exhibits consistent daily activity, with charge and discharge energy averaging around 1200 kWh per day. The bar chart in Figure 5(a) complements Table 2 showing temporal variability and charge–discharge balance, highlighting patterns less evident in the table. For example, April 3 records relatively high discharge compared to charging, coinciding with moderate hydrogen production and electricity export—indicating a shift toward supporting downstream loads rather than storage. Conversely, net charging days align with surplus RE availability. The SOC trend in Figure 5(b) oscillates between 20% and 35%, underscoring the battery's role as a flexible energy buffer. Together, these plots illustrate the MFCS's capacity to shift energy temporally, reduce grid dependence, and adapt to supply–demand fluctuations.

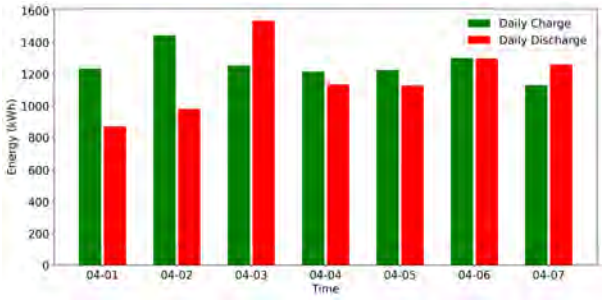

(a) Daily battery charge and discharge energy.

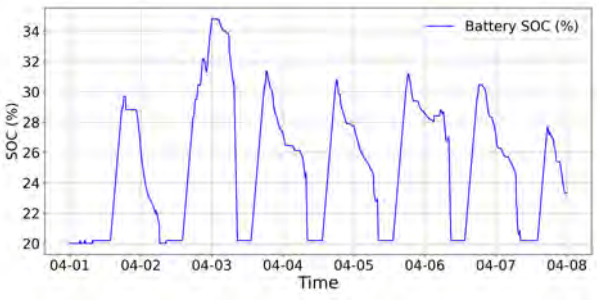

(b) Battery state of charge (SOC) over time.

Figure 5: Battery energy flow and SOC dynamics over the simulation period.

4.2 Sensitivity Analysis

To assess the robustness and flexibility of the MFCS design under changing operational conditions, we perform a series of sensitivity experiments. These experiments vary key parameters, including electricity price, EV demand intensity, hydrogen demand, and component sizing to evaluate their impact on system-level energy

flows and financial performance. While the simulation captures stochastic dynamics, numerical results presented in this subsection are averaged over 50 runs to ensure that each scenario reflects representative system behavior and enables consistent comparison across experimental conditions.

4.2.1 Impact of Electricity Price Fluctuations on System Profitability

Here, we examine how changes in electricity prices affect grid interactions, H_2 production, and the station's overall performance. Table 3 summarizes the absolute values across a price change range of -20% to $+20\%$ relative to the base case. Percentage-based comparisons below are derived from these values to provide a clearer interpretation of system sensitivity.

Table 3: Sensitivity analysis of electricity price on MFCS operation.

(%) Change	Power (kWh) Purchased for			Grid Interaction		H_2 (kg)	Revenue and Cost Breakdown ($)				
	EVs	H_2	Battery	Buy	Sale	Production	EV Rev	H_2 Rev	Grid Sale	Grid Buy	Net
-20%	11.98	47092.50	12236	59340.48	445.38	989.04	2785.88	28063.91	261.58	-127.62	30983.75
-15%	17.97	48073.33	10469	58560.30	330.18	1009.64	2771.97	27955.67	199.12	-81.09	30845.67
-10%	23.43	48382.50	9576	57981.93	276.77	1016.13	2757.56	27873.32	144.17	-58.43	30716.62
-5%	27.14	48475.00	9063	57565.14	311.57	1018.08	2748.26	27764.48	119.13	-45.87	30586.00
0%	28.66	48650.83	8806.5	57486.00	401.19	1021.77	2741.75	27744.00	113.75	-40.40	30559.10
5%	32.94	48220.00	8540.5	56793.44	522.78	1012.72	2727.55	27516.41	75.06	-34.37	30284.66
10%	51.91	47180.00	8303	55534.91	595.80	990.88	2679.49	27175.41	83.33	-29.54	29908.70
15%	53.47	45409.17	8236.5	53699.13	716.26	953.69	2641.82	26565.33	91.05	-28.84	29269.36
20%	49.08	40544.17	8160.5	48753.75	775.52	851.51	2581.03	25082.44	63.94	-27.48	27699.94

A key observation is the nonlinear relationship between electricity price and grid purchases. As prices increases, purchases fall from 59.3 MWh (11.98 + 47,092 + 12,236 kWh) at -20% to 48.8 MWh at $+20\%$. This drop is mainly driven by a 13.9% reduction in power for H_2 production (47,092 $\rightarrow$ 40,544 kWh), confirming it as the most price-sensitive activity. In contrast, grid electricity for EVs increases from 11.98 kWh to 49.08 kWh, a 309% rise, reflecting reliance on grid power to meet EV demand as RE is shifted toward H_2. On the revenue side, both H_2 and EV services show similar declines of about 10.8% and 11%. The fall in H_2 revenue stems from reduced grid-powered production, which increases dependence on RE and limits surplus available for export. Consequently, grid sale revenue drops from \$261.58 to \$63.94.

The net result is a notable profit compression: from a peak of \$30,984 at -20% price to \$27,700 at $+20\%$, an $\sim 11\%$ decline. This occurs despite stable or reduced energy use, highlighting the strong influence of electricity pricing on MFCS economics.

While the MFCS remains operationally robust across varying prices, profitability is highly sensitive to increases. Strategies such as dynamic scheduling or real-time price-based dispatch could mitigate losses, while long-term investments in RE capacity and storage would provide greater insulation from grid volatility and enhance economic resilience.

4.2.2 System Sensitivity to Arrival Patterns and Charging Capacity

This section investigates how fluctuations in EV arrival rates and charger availability influence the MFCS operation. Figure 6 presents the system's response to changing arrival rates assuming a fixed 10-charger setup, while Table 4 shows performance metrics across varying charger counts.

Figure 6 shows that as EV arrivals increase from -20% to $+20\%$, the number of EVs served rises from 279 to 388, and EV charging revenue climbs from \$2376 to \$3134 (Figure 6a). However, this improvement in throughput leads to performance degradation. The percentage of demand met falls from 96.7% to 89.5%, while average wait time increases from 4.47 to 7.30 minutes. Abandoned EVs also spike from 0 to 21 as arrival rates climb (Figure 6b). These results highlight the infrastructure's diminishing ability to maintain service quality under growing load, emphasizing the trade-off between utilization and customer satisfaction.

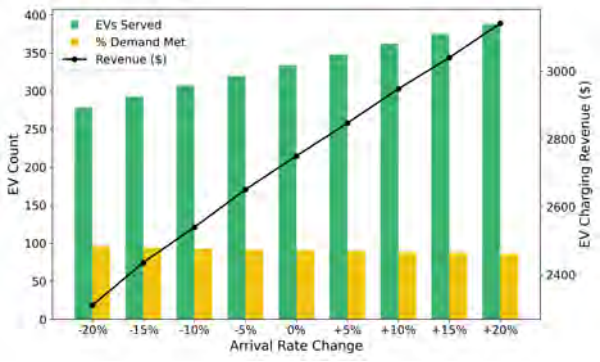

(a) EVs Served, % Demand Met, and Revenue

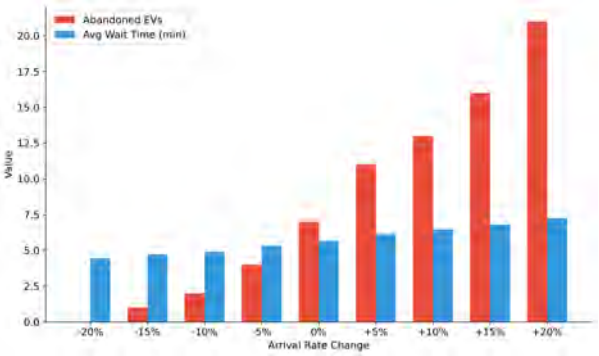

(b) Abandoned EVs and Avg Wait Time

Figure 6: Sensitivity of MFCS performance to arrival rate changes (10 chargers).

Table 4 reveals a saturation point in service gains as charger capacity increases. While moving from 2 to 7 chargers greatly improves demand coverage (from 39.75% to 90.8%) and significantly reduces wait time and abandonment, additional chargers beyond 9 offer diminishing returns. This performance plateau supports the use of 10 chargers as a practical baseline configuration, balancing cost and user satisfaction.

Table 4: Sensitivity of charger count on EV performance.

No. of Chargers	EV Power Supply (kWh) from RE	Battery	Grid	Fuel Cell	Total Supplied	% Demand Met	Avg Wait Time (min)	Aban. EVs
2	4285.78	900.80	22.05	1.59	5210.22	39.75	13.27	219.86
5	8076.94	2141.88	24.72	1.88	10245.41	78.10	9.54	77.98
7	9268.73	2623.12	28.66	1.92	11922.43	90.80	7.49	30.38
9	9755.71	2845.48	35.83	1.92	12638.94	96.21	6.05	9.46
11	9904.56	2911.22	39.68	1.93	12857.38	97.84	5.37	2.22
13	9933.71	2926.42	40.60	1.93	12902.66	98.17	5.09	0.46

4.2.3 Evaluating Capacity Constraints for H_2 Demand Growth

To test the MFCS's ability to accommodate rising H_2 demand, the baseline H_2 requirement was incrementally increased by up to 20%. At baseline, unmet demand was minimal (1.6%, or 27.8 kg), but as demand scaled, system limitations became evident. At 10% and 20% increases, unserved demand rose to 5.2% (98.5 kg) and 9.2% (187.7 kg), respectively, as shown in Figure 7. This non-linear growth signals bottlenecks tied to electrolyzer throughput, storage capacity, and the prioritization of EV charging over H_2 production.

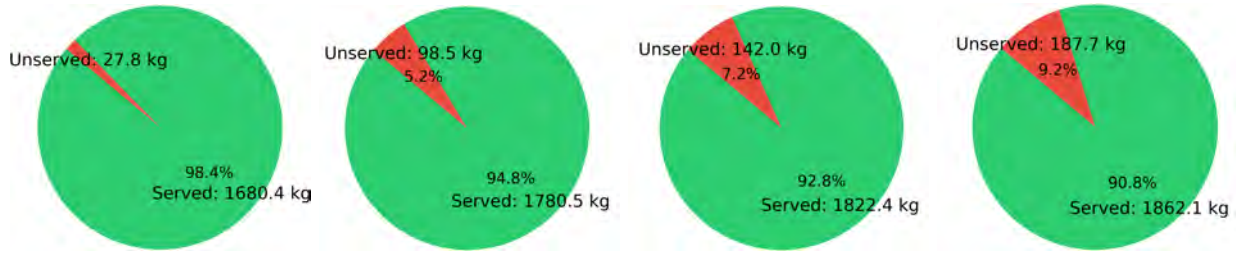

(a) 0% Increase (b) 10% Increase (c) 15% Increase (d) 20% Increase

Figure 7: H_2 demand fulfillment under different demand increase scenarios.

Despite this, the MFCS still increased its total H_2 output from 1680.4 kg at baseline to 1862.1 kg under 20% higher demand, highlighting the system's elasticity. However, the rising shortfall translates to lost revenue, which grows from about $458 to about $3100, underscoring the economic cost of capacity constraints. These findings reveal the boundaries of current system settings. The MFCS performs robustly under baseline and moderate increases, yet significant future growth in HFCV usage may necessitate capacity expansion or more adaptive dispatch strategies to maintain service quality and economic efficiency.

5 CONCLUSION

This paper presents a simulation-based operational analysis of MFCS integrating RE generation, battery storage, H_2 production, and grid-market participation. Using 5-minute resolution over a 7-day horizon, the model provides insights into interactions between energy vectors and transportation services. Baseline results demonstrate the MFCS's ability to achieve high RE utilization and sustained service for both EVs and HFCVs, while maintaining economic viability through intelligent grid interaction. Experiments highlight trade-offs and performance thresholds: electricity price volatility affects profitability; rising EV arrivals strain infrastructure and reduce service quality; and adding chargers beyond nine yields diminishing returns. Moderate HFCV demand growth remains manageable, but further scaling requires upgrades in electrolyzer capacity, storage, or dispatch strategies. Future work may include incorporating stochastic demand models, such as time-varying Poisson arrivals, to capture uncertainty; integrating reinforcement learning for adaptive dispatch under uncertainty; extending the model to multi-node MFCS networks for inter-hub coordination; and embedding long-term dynamics, such as endogenous demand growth or dynamic pricing, to support infrastructure planning under evolving regulatory and market conditions.

ACKNOWLEDGMENTS

This work was supported in part by the U.S. Department of Energy's Advanced Research Projects Agency-Energy (ARPA-E) under the project (#DE-AR0001780) titled "A Cognitive Freight Transportation Digital Twin for Resiliency and Emission Control Through Optimizing Intermodal Logistics" (RECOIL).

REFERENCES

Ait Alla, A., E. Broda, M. Teucke, L. M. Steinbacher, S. Oelker, and M. Freitag. 2024. "Simulation-Based Analysis of Hydrogen Refuelling Station to Support Future Hydrogen Trucks and Technological Advances". In *2024 Winter Simulation Conference (WSC)*, 242–251 https://doi.org/10.1109/WSC63780.2024.10838915.

Benz, P., and M. Pruckner. 2023. "Lightweight Smart Charging vs. Immediate Charging with Buffer Storage: Towards a Simulation Study for Electric Vehicle Grid Integration at Workplaces". In *2023 Winter Simulation Conference (WSC)*, 922–933 https://doi.org/10.1109/WSC60868.2023.10407436.

Bogdanov, D., M. Ram, S. Khalili, A. Aghahosseini, M. Fasihi, and C. Breyer. 2024. "Effects of Direct and Indirect Electrification on Transport Energy Demand During the Energy Transition". *Energy Policy* 192:114205 https://doi.org/10.1016/j.enpol.2024.114205.

Choukulkar, A., Y. Pichugina, C. T. M. Clack, R. Calhoun, R. Banta, A. Brewer *et al*. 2016. "A New Formulation for Rotor Equivalent Wind Speed for Wind Resource Assessment and Wind Power Forecasting". *Wind Energy* 19(8):1439–1452 https://doi.org/10.1002/we.1929.

Ghirardi, E., G. Brumana, G. Franchini, N. Aristolao, and G. Vedovati. 2024. ""The Role of Hydrogen Storage and Electric Vehicles in Grid-Isolated Hybrid Energy System with High Penetration of Renewable"". *Energy Conversion and Management* 302:118154 https://doi.org/10.1016/j.enconman.2024.118154.

Huang, C.-J., M.-T. Huang, and C.-C. Chen. 2013. "A Novel Power Output Model for Photovoltaic Systems". *International Journal of Smart Grid and Clean Energy* 2(2):139–147.

Koenemann, L., A. Bensmann, J. Gerster, and R. Hanke-Rauschenbach. 2024. "Dispatch of Decentralized Energy Systems Using Artificial Neural Networks: A Comparative Analysis With Emphasis on Training Methods". *Energy Conversion and Management: X* 24:100730 https://doi.org/10.1016/j.ecmx.2024.100730.

Lee, S., L. Al-Ghussain, M. Alrbai, and S. Al-Dahidi. 2024. "Integrating Hybrid PV/Wind-Based Electric Vehicles Charging Stations With Green Hydrogen Production in Kentucky Through Techno-Economic Assessment". *International Journal of Hydrogen Energy* 71:345–356 https://doi.org/10.1016/j.ijhydene.2024.05.053.

Meier, K. 2014. "Hydrogen Production With Sea Water Electrolysis Using Norwegian Offshore Wind Energy Potentials: Techno-Economic Assessment for an Offshore-Based Hydrogen Production Approach With State-of-the-Art Technology". *International Journal of Energy and Environmental Engineering* 5(2):104 https://doi.org/10.1007/s40095-014-0104-6.

Ramkumar, M. S., J. Subramani, M. Sivaramkrishnan, A. Munimathan, M. Goh Kah Ong, and M. M. Alam. 2025. "Optimal Energy Management for Multi-Energy Microgrids Using Hybrid Solutions to Address Renewable Energy Source Uncertainty". *Scientific Reports* 15(1):7755 https://doi.org/10.1038/s41598-025-90062-8.

Shi, T., F. Zhao, H. Zhou, and C. Qi. 2024. "Research on Intelligent Energy Management Method of Multifunctional Fusion Electric Vehicle Charging Station Based on Machine Learning". *Electric Power Systems Research* 229:110037 https://doi.org/10.1016/j.epsr.2023.110037.

Sing, K., P. Mertiny, and M. Pruckner. 2022. "Modeling and Simulation to Improve Real Electric Vehicles Charging Processes by Integration of Renewable Energies and Buffer Storage". In *2022 Winter Simulation Conference (WSC)*, 867–878 https://doi.org/10.1109/WSC57314.2022.10015432.

U.S. Energy Information Administration 2025. "Ẅholesale Electricity Market Data – CAISO". https://www.eia.gov/electricity/wholesalemarkets/data.php?rto=caiso. Accessed 19th June 2025.

Valipour, E., A. Babapour-Azar, R. Nourollahi, R. Khanjani-Shiraz, and M. Römer. 2024. "Risk-driven Optimal Scheduling of Renewable-oriented Energy Hub Under Demand Response Program and Energy Storages: A Novel Entropic Value-at-Risk Modeling". *Sustainable Cities and Society* 107:105448 https://doi.org/10.1016/j.scs.2024.105448.

Wang, Y., J. Liu, and Z. Qu. 2024. "Multi-Stage Collaborative Planning of Electricity-Hydrogen-Transportation Coupling Network Considering Carbon Emission Reduction". *Electric Power Systems Research* 228:110071 https://doi.org/10.1016/j.epsr.2023.110071.

Weather Underground 2025. "Personal Weather Station Dashboard: KCASANFR2105 (San Francisco)". https://www.wunderground.com/dashboard/pws/KCASANFR2105. Accessed 19th June 2025.

Xiao, G., H. Liu, and J. Nabatalizadeh. 2025. "Optimal Scheduling and Energy Management of a Multi-Energy Microgrid with Electric Vehicles Incorporating Decision Making Approach and Demand Response". *Scientific Reports* 15(1):5075 https://doi.org/10.1038/s41598-025-88776-w.

Zhang, B., Z. Chen, L. Zang, P. Guo, and R. Miao. 2025. "Coordinated Battery Charging and Swapping Scheduling of EVs Based on Multilevel Deep Reinforcement Learning for Urban Governance". *IEEE Transactions on Intelligent Transportation Systems* 26(3):3784–3798 https://doi.org/10.1109/TITS.2024.3524673.

Zheng, B., and W. Wei. 2025. "Real-Time Peer-to-Peer Energy Trading for Networked Multi-Energy Systems With Hybrid Energy Storage". *Journal of Energy Storage* 105:114530 https://doi.org/10.1016/j.est.2024.114530.

Zheng, Y., Y. Wang, and Q. Yang. 2025. ""Market Mechanism Enabling Electric Vehicle Grid Integration: A Critical Review on Operational Frameworks, Service Provisions and Optimization Techniques"". *Sustainable Cities and Society* 125:106347 https://doi.org/10.1016/j.scs.2025.106347.

AUTHOR BIOGRAPHIES

JEREMIAH GBADEGOYE is a Ph.D. student in the Department of Industrial and Systems Engineering, University of Tennessee, Knoxville. His research interests include logistics and supply chain optimization, energy management systems, and simulation modeling of complex systems. His e-mail address is Jgbadego@vols.utk.edu.

YANG CHEN is a Research Scientist in the Computational Urban Sciences Group within Computational Sciences and Engineering Division at Oak Ridge National Laboratory. His research interests include machine learning, optimization and simulation, with applications in power grid, urban infrastructure, and healthcare. His email address is cheny4@ornl.gov.

OLUFEMI A. OMITAOMU is a Distinguished R&D Staff and Group Leader in Computational Urban Sciences group at Oak Ridge National Laboratory. His research expertise includes disaster risk analysis and urban systems resilience, energy infrastructure siting and analysis, artificial intelligence in critical infrastructure systems, and anomaly detection in complex system. He received his Ph.D. in Industrial Engineering from the University of Tennessee, Knoxville. He is a senior member of IEEE and IISE; member of ACM and AAAI. His email address is omitaomuoa@ornl.gov.

XUEPING LI is a Professor and Dan Doulet Faculty Fellow of Industrial and Systems Engineering and the Director of the Ideation Laboratory (iLab) and co-Director of the Health Innovation Technology and Simulation (HITS) Lab at the University of Tennessee - Knoxville. He holds a Ph.D. from Arizona State University. His research areas include complex system modeling, simulation, and optimization, with broad applications in supply chain logistics, healthcare, and energy systems. He is an IISE Fellow and a member of IEEE, ASEE, and INFORMS. His e-mail address is Xueping.Li@utk.edu. His website is https://xli.tennessee.edu/.